Lasers in Manufacturing Conference 2019

Optimized Temperature Distribution for Laser Hardening with Freeform Mirrors

Thomas Bergs[a], Martin Schulz[b*], Stefan Gräfe[b], Jan Riepe[b], Kristian Arntz[b]

[a]*Laboratory for Machine Tools and Production Engineering (WZL) of RWTH Aachen University, Campus-Boulevard 30, 52074 Aachen, Germany*
[b]*Fraunhofer Institute for Production Technology IPT, Steinbachstraße 17, 52074 Aachen, Germany*

Abstract

Laser beam shaping by the usage of freeform mirrors for laser hardening is a known technology which has been used for CO2-Lasers. Nevertheless, due to developments in manufacturing technologies and computer simulation the industrial relevance has increased recently. By now, it is possible to manufacture freeform mirrors precise enough for the diode laser wavelength. With these mirrors, complex intensity distributions can be generated. Combined with a solution of the Inverse Heat Conduction Problem, the temperature distribution in the process zone can be designed according to the process necessities. This study will compare the results of three different profiles which were designed to optimize the process. The first optic generates a rectangular isothermal profile. The second is a rectangle with a reduction of temperature in the direction of the movement to avoid grain growth. The third is optimized to increase the desired compressive residual stresses.

Keywords: Freeform optics; Optimized temperature distribuition; Laser hardening

1. State of the art

1.1. Process Principle

In laser hardening, the laser is directed to the surface of a steel part to generate a hard surface layer. When the temperature of the material reaches austenitization temperature, carbon can solute from a carbon rich phase into austenite. The temperature afterwards drops quickly due to the heat conduction from a surface layer into the bulk material. High cooling rates trap the carbon in the crystal forming martensite.

The laser power is usually regulated by a pyrometer to assure a temperature range between austenitization and melting temperature at the surface. The depth of the hardening track depends on whether the temperature cycle at the laser spot was high enough to form austenite and was held long enough for carbon to diffuse before being cooled down fast enough. Besides the feed rate and the laser power, the process results are thereby depending on the intensity distribution on the surface of the substrate causing the temperature field. (Schmitz-Justen 1986; Berns and Theisen, 2008; Graf and Hügel, 2009)

* Corresponding author. Tel.: +49-241-8904-560; fax: +49-241-8904 -6560.
E-mail address: martin.schulz@ipt.fraunhofer.de.

1.2. Optical Elements for Optimized Temperature Distributions

Optical elements for laser beam shaping for high-power continuous-wave applications may be separated in four categories.

The first category was applied in the beginning of laser hardening when the laser beams were not actively shaped. The power distribution was only determined by the type of laser source and its setup. Lenses or mirrors can be used for guiding the laser beam or changing its size, but the relative intensity distribution is not changed. These distributions are e.g. Gaussian or in the case of a High Power Diode Laser (HPDL) the slow and fast axis of the beam. For Laser hardening they have several flaws; the maximum temperature is reached at a small point in the center of the hardened track only. Large amounts of energy are spread in places where the austenitization temperature is not reached. This energy will not directly contribute to the process.

In the second category, the laser beams are homogenized. There are several ways to homogenize a laser beam. One of the most commonly used is the Fly-Eye-Homogenizer. This homogenizer arranges small images of the beam to generate a homogeneous beam (Sandven, 1991). Another option are the so-called Field Mappers, which rearrange fields of the incoming beam to generate a more homogeneous output beam. The most often used homogenizer however is the multimode fiber producing a homogeneous round spot. By now, rectangular shaped fibers are available (Blomster and Blomqvist, 2007) generating rectangular shaped beams. The temperature distribution of a homogeneous intensity distribution is more homogeneous but still overheats in the middle of the spot (Geissler, 1993). Nevertheless, it is the most used intensity distribution and state of the art in the industry.

The third category would be standard optical elements, which generate their specific typical intensity distribution. While the kind of intensity distribution is determined by the optical elements, the characteristics of the intensity distributions can be used to generate a temperature field, which has positive effects on the process. The most prominent example of this category was made by Burger (Burger, 1988). Burger approximated the necessary intensity distribution to form a homogeneous temperature field by adapting the movement of a laser scanner. Other examples are the usage of axicons, which produce circles in the focal area. These were investigated by several authors (Laskin, 2014; Wellburn et al. 2014; Sundqvist et al., 2017). Most of these approaches try to achieve a homogenous surface temperature.

The fourth category are complex optical elements, which allow to freely design the intensity distributions. The degree of freeform of these distributions is only limited by the quality of the laser source and the optical elements. These optical elements may be diffractive optical elements (DOE) or freeform mirrors. While DOE allow to generate higher-contrast images, they depend on a well defined coherent laser source. Approaches to use these to optimize the laser hardening process were done by several authors (Leung et al., 2007; Noden, 2000; Primartomo, 2005 or Hagino et al., 2010). The authors mostly used the additional degree of freedom to generate homogenous surface temperatures. Only Primartomo mentioned a higher temperature at the beginning to optimize the process. Freeform Mirrors can easily be combined with high power diode laser systems. For an understanding of the principle, the mirrors might be interpreted as field mappers with infinitesimal small fields. Other current developments in complex beam shaping devices for high power applications are high power deformable mirrors (Pütsch, 2016), high power microelectronic membranes (mems) (Hofmann et al., 2016) and scanners in combination with modulated high power laser (Martínez et al., 2016) which allow to adapt the intensity profile online.

The elements of the fourth category allow to generate complex shaped intensity distributions. Combined with an approximation of the inverse heat conduction problem, it is possible to define temperature fields optimized for the laser hardening process. Until now, this technique was mostly used to generate homogeneous surface temperatures.

1.3. Solutions of the Inverse Heat Conduction Problem

The process results are depending on the temperature field, which itself is determined by the intensity distribution, feed rate, laser power and material properties. Hence, to optimize the process temperature field the necessary intensity distribution has to be calculated. This mathematical problem is called Inverse Heat Conduction Problem. An analytical solution for the Inverse Heat Conduction Problem is unknown, but there are several ways to numerically approximate the solution. One option, for example, is the Laser Tool Box for Matlab by Römer (Römer and Huis in ’t Veld, 2010). The empirical part of this paper is based on the results shown by Völl et al. (Völl et al., 2016). The visualization of the temperature fields in the next chapter is done with another approach. The temperature field is calculated by Gaussian sources, which can be superposed for the steady state.

2. Derivation of Optimized Temperature Fields

2.1. Introduction

The state of the art allows to calculate the necessary intensity distribution for a given temperature field. This static intensity distribution than can be generated with a freeform mirror or diffractive optical elements (DOE). This raises the question, how an optimized temperature field should be shaped to improve the process. In the following chapter, candidates for such an optimized temperature field will be discussed.

2.2. Isothermal Surface Temperature

The effects of an isothermal process can be separated in the effect in the direction of motion and the effect perpendicular to it. Acommon used homogenized intensity distribution generates an overheating in the middle of the spot. Perpendicular to the feed motion this causes higher surface temperature in the middle, which again causes higher hardening depths forming a lens-like hardened track. This can be reduced by a correction of the temperature in the perpendicular direction. The maximum process temperature on the surface is restricted due to the melting temperature. Normally the maximum temperature is reached at a small spot only. By using a profile that homogenizes the temperature in the direction of motion this maximum temperature can take effect in a larger area. Due to the larger high temperature area on the surface, the temperature in a certain depth is reached quicker. The feed rate can increase and so the productivity raises. Faster heat up rates also will activate more crystal seeds, which should result in finer grains. As a negative effect, the surface temperature is hold on a high level for a longer time. This will cause grain growth and should be avoided. Another negative effect which was described by Küpper (Küpper, 1996) is the higher necessary laser power of an isothermal process due to the higher temperature gradients. To avoid the negative effects of the isothermal process, either the feed rate has to be adapted or the surface temperature has to be reduced. In further discussion, this profile will be called isothermal profile.

2.3. Shaping the Temperature Distribution to Reduce Grain Growth

To avoid the drawbacks of the isothermal process it is suggested that the surface temperature in the profile starts with a high value and then decreases. The perpendicular temperature distribution may again be constant over the length. To determine which function the decreasing temperature should follow time-temperature-transformation diagrams are used. The formula for a constant grain growth is fitted to the values given in the “Atlas zur Wärmebehandlung der Stähle” (Orlich et al., 1973). To avoid melting during the process, the temperature is limited to 1225 °C. Thereby the temperature distribution in figure 1 (left) is suggested. The intensity distribution shown in figure 1 is similar to the isothermal solution, which was suggested by Burger (Burger, D., 1988) but has a steeper gradient to form the temperature field. The temperature profile is plotted for a feed rate of 400 mm/min. The material is 42CrMo4. This surface temperature field should reproduce most of the benefits of the previous isothermal surface temperature and avoid the negative effect of grain growth. In further discussion, this profile will be called reduced-grain-growth profile.

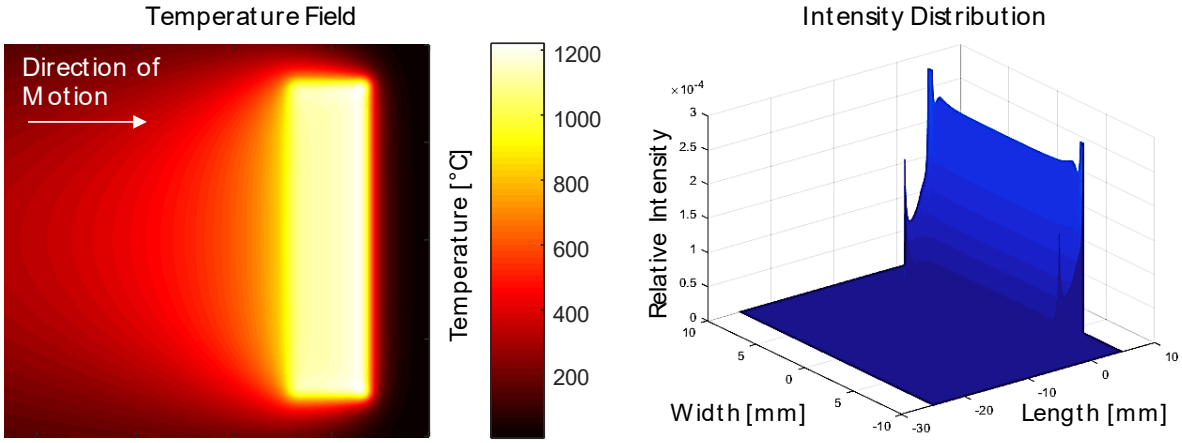

Fig. 1. Temperature field (left) and intensity distribution (right) suggested to reduce grain growth.

2.4. Shaping the Temperature Distribution to Optimize Residual Stresses

Besides the high hardness, the resulting high compressive residual stresses are one of the main advantages of laser hardening compared to other surface hardening techniques. The compressive residual stresses are induced by the formation of the martensitic phase due to the larger volume of the phase (Sandven, 1991). There are two phenomena reducing this positive effect: Thermal Tensions and Transformation Ductility.

At high temperature, the thermal expansion of the material causes compression in the hardened zone. In this area, the compression can overcome the thermally reduced compressive strength and the material deforms. When the material is cooled to room temperature, it is stretched and tensions occur (Kostov, 2014; Besserdich, 1993). To avoid the effect the material should be cooled as fast as possible and high temperatures as well as holding times should be avoided. Additionally sharp edges of the temperature field will cause high stresses in the material. To reduce the described effects, the authors suggest to angle the previously described temperature field and round the tip of the thereby generated arrow. The arrow allows to spread the expanded high temperature areas over a wider range. This way the individual expansions will not sum up to reach the high compression stress values which than overcome the thermally reduced compressive strength. This is than combined with the decreasing temperature of the temperature field discussed before.

By the use of the arrow shaped temperature profile, the second effect, Transformation Ductility, can also be reduced. The area which is surrounded by the arrow is held above martensitic start temperature. Therefore, the increasing ductility during transformation (Kostoc, 2014; Besserdich, 1993), during the austenite-martensite formation in this case, will not interact with the thermal tensions generated by the high temperature areas.

The resulting temperature field and intensity distribution is shown in figure 2. The calculation was made with a feed rate of 400 mm/min. The material is 42CrMo4 and the maximum temperature 1225°C. It should reduce the grain growth like the before discussed temperature profile and additionally optimize the residual stresses. In further discussion, this profile will be called arrow profile.

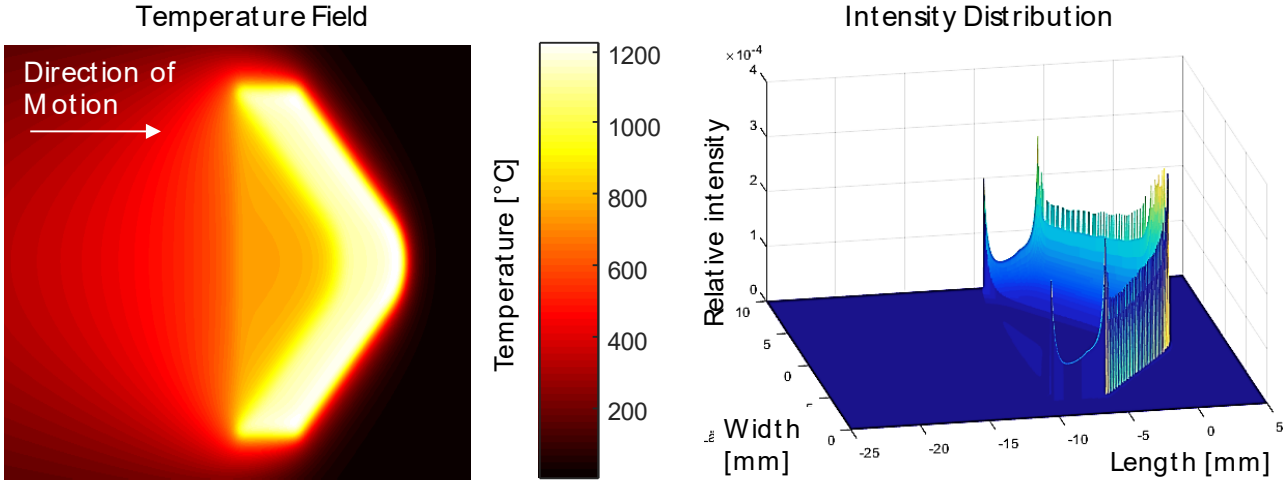

Fig. 2. Temperature field and intensity distribution suggested to generate higher compressive stresses.

3. Experimental procedure

The intensity distribution as well as the shape of the mirrors was calculated by the “Lehrstuhl für Technologie optischer Systeme (TOS)” of the RWTH-Aachen University. The mirrors were manufactured by the company Innolite GmBh using oxide free, high conductivity (OFHC) copper. The used laser source was diode laser by Laserline with a maximum laser power of 5000 W. The process was regulated by a two-color pyrometer of the company Dr. Mergenthaler GmbH & Co. KG. The temperature of the control cycle was set to 1225°C. The pyrometer measurement spot was set to the position where the highest temperature is expected. The handling system was the CNC lathe »RNC 400 Laserturn« by Monforts Werkzeugmaschinen GmbH with a special laser tool manufactured to hold the mirror. Shafts with a diameter of 50 mm made of quenched steel 42CrMo4 were hardened. The process feed rate for the isothermal profile and the arrow profile was 400 mm/min while the reduced-grain-growth profile was processed at low feed rates of 96mm/min. Each process was reproduced at least three times. Metallographic analysis were done of each trail to measure the hardening depth and width, measure the shape of the hardened area and analyze the microstructure via optical microscope. The deformation of the shape was measured with an optical measurement tool Alicona Infinite focus G5.

4. Results

The process with the isothermal temperature profile is known from literature and has already been presented (Klocke et al., 2017). Therefore, it will be used as benchmark. The further results will focus on the before mentioned arrow profile. The mean power is 2108 W for the isothermal profile, 2191 W for the reduced-grain-growth profile and 2320 W for the arrow profile. The highest deviation from the mean value of the mean power of each tryout is about 60 W and thereby around 3% of the lowest mean value. The mean value of the arrow profile is 10 % more than the one of the isothermal profile. Nevertheless, the consumed energy of the process with the reduced-grain-growth is much higher due to the extended interaction time. The four times higher energy consumption and the longer processing time due to the approximately four times reduced feed rate seem to make the grain growth profile uneconomical. The metallographic analysis of the hardened tracks produced with the arrow profile (three repetitions) as well as one of the isothermal profile processes can be seen in figure 3 (maximum Temperature 1225°C, feed rate 400 mm/min). The martensitic transformation can be seen easily due to the good contrast after etching. The arrow profile generates a 28 % deeper hardened track. The change in hardening depth during arrow profile process lies in an insignificant range of 60 µm. The hardened area is more lens-shaped compared to one generated with the isothermal profile. This is probably due to the longer holding time in the center of the track, which was done to avoid phase transformation in the high stress area. The track width is 5 % shorter than the isothermal profile.

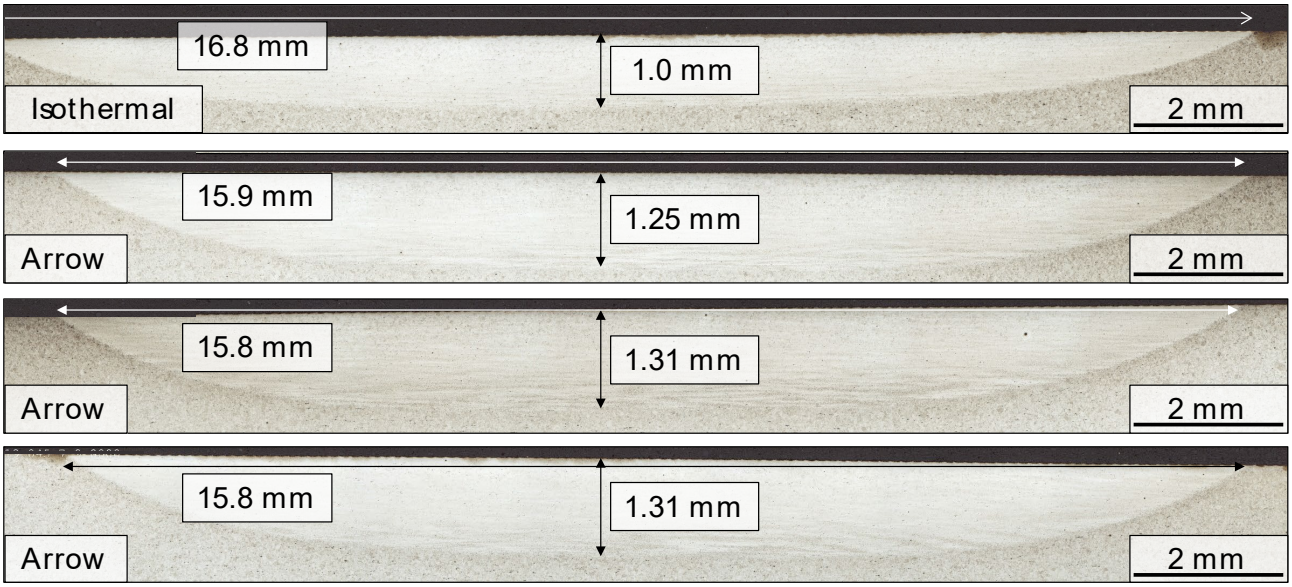

Fig. 3. Metallographic analysis of isothermal process (top) and three optimized hardening tracks produced with a freeform mirror

In figure 4, the microstructure next to the surface of the isothermal and the arrow profile are shown. In both cases, martensitic microstructure developed. The feed marks of the turning process can be seen. The grains are fine. These are indicators that no negative thermal effects appeared. The oxide layer of the process with the arrow profile is slightly thicker.

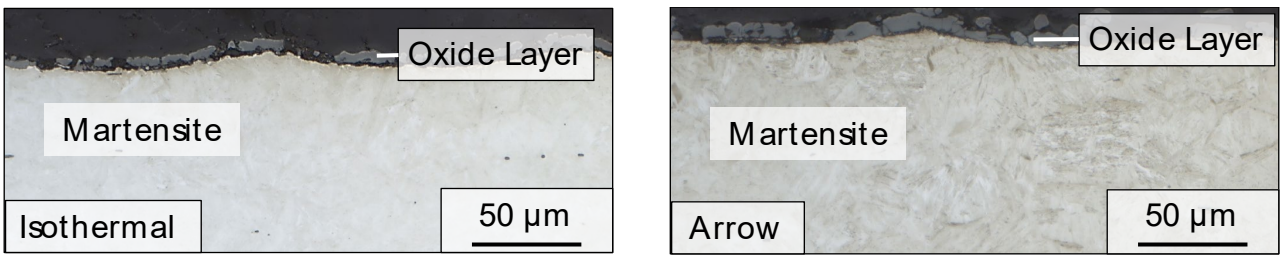

Fig. 4. Microstructure of the isothermal profile (left) and the arrow profile (right).

The residual stresses will lead to a deformation over the width of the track. This deformation including the oxidation layer was measured with an Alicona Infinite focus G5. The data was processed with Matlab to reduce noise and filter out the roughness of the turning process. The resulting deformation over the width of the track is shown in figure 5. The process with the isothermal profile shows a deformation of 18 µm while the height of the arrow shaped profile exceeds 30 µm. This is much more than the deeper hardened track of around 20 % would explain. This also cannot be explained by the height of the oxide layer, which is only slightly thicker as can be seen in figure 3.

It is assumed that the isothermal profile thermal tensions evoke which compensate the compressive stresses in the middle of the track. Thereby the compression in the center of the track is reduced generating a plateau. In comparison, the deformation of the arrow profile steadily increases until it reaches the maximum in the middle of the track and then decreases. Therefore, the compressive residual stresses are not reduced by plastic deformation. As was said before, higher compressive tensions should lead to higher wear resistance.

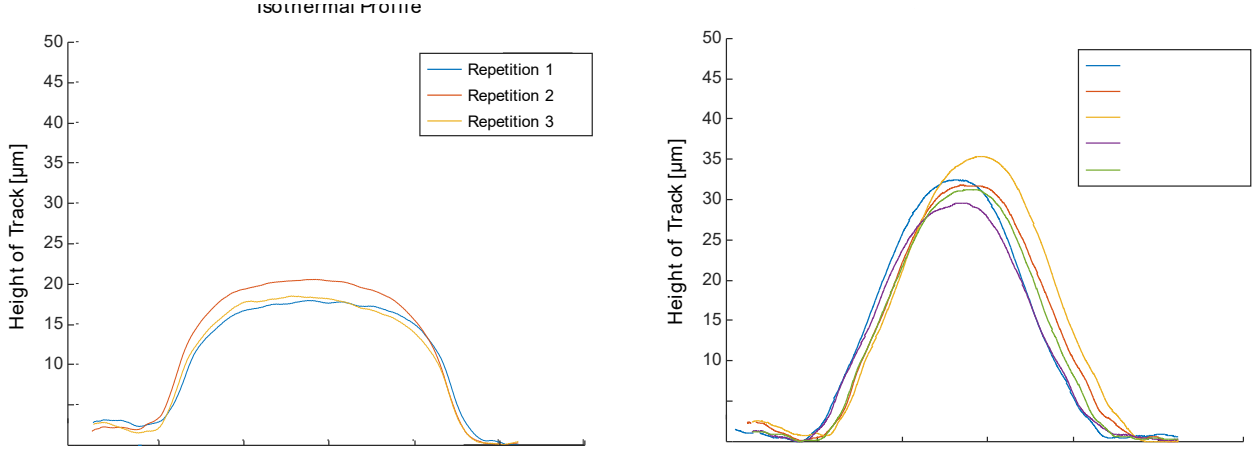

Fig. 5. Deformation over the width of the track for isothermal profiles (left) and arrow shaped profiles (right).

5. Discussion and Conclusion

The intensity distributions for laser hardening can be separated in four different categories depending on the level in which the intensity is actively shaped to optimize the temperature field. Despite the technical possibilities, this degree of freedom is seldom used to optimize the temperature of the process. Therefore, the authors suggested two profiles besides the already known isothermal profile.

The chosen parameter set for the profile for reduced-grain-growth seems to be unproductive for the usage of the quenched 42CrMo4. Nevertheless, the profile might be promising on materials with longer diffusion paths like globular-annealed materials.

The arrow profile shows 20% higher hardening depth and the deformation of the surface indicates that the positive compressive residual stresses were successfully optimized. No negative effects occurred in the surface microstructure and compared to the isothermal profile only 10 % more power was necessary. However, whether the hardened track really shows a higher wear resistance has to be practically evaluated in future studies.

Future studies will have to clarify whether these benefits may also be reached by adapting other parameters of the state of the art top-hat profile or the isothermal profile like the length of the track, the feed rate or the maximum surface temperature. In other words, the potential of the optimized profiles of the fourth category has to be validated against the whole process window of the state of the art optical elements to justify the higher complexity.

Acknowledgements

The Federal Ministry of Education and Research (BMBF), Berlin, Germany, is acknowledged for financial support within the project Nano-DPP (grant number 13N13476). The authors would like to thank the Innolite GmBh for providing the freeform mirror and the Chair for Technology of Optical Systems (TOS) for the design of it.

References

Bachmann, F., W. Rath, and V. Auerbach, 2004, Der Einsatz von Hochleistungs-Diodenlasern zum Härten und Beschichten∗: HTM Härtereitechnische Mitteilungen, v. 59, no. 3, p. 217–224.

Berns, H., and Theisen, 2008, Eisenwerkstoffe - Stahl und Gusseisen: Berlin, Heidelberg, Springer Berlin Heidelberg.

Besserdich, G., 1993, Untersuchungen zur Eigenspannungs- und Verzugsausbildung beim Abschrecken von Zylindern aus den Stählen 42 CrMo 4 und Ck 45 unter Berücksichtigung der Umwandlungsplastizität, Dissertation, Karlsruhe, 300p.

Blomster, O., and M. Blomqvist, 2007, Square formed fiber optics for high power applications. in F. Vollertsen, ed., Lasers in manufacturing 2007: Proceedings of the Fourth International WLT-Conference Lasers in Manufacturing, LIM 2007, Munich, Germany, June 18th - 22nd, 2007: Lasers in Manufacturing 2007, LIM, International WLT-Conference on Lasers in Manufacturing, 4: Stuttgart, AT-Fachverl., p. 817–819.

Burger, D., 1988, Beitrag zur Optimierung des Laserhärtens, Dissertation, Universität Stuttgart, Stuttgart.

Geissler, E., 1993, Mathematische Simulation des temperatur-geregelten Laserstrahlhärtens und seine Verifikation an ausgewählten Stählen, Dissertation, Universität Erlangen-Nürnberg, Erlangen, 175p.

Graf, T., and H. Hügel, 2009, Laser in der Fertigung: Strahlquellen, Systeme, Fertigungsverfahren: Wiesbaden, Vieweg+Teubner Verlag / GWV Fachverlage GmbH, Wiesbaden, Online-Ressource.

Hagino, H., S. Shimizu, H. Ando, and H. Kikuta, 2010, Design of a computer-generated hologram for obtaining a uniform hardened profile by laser transformation hardening with a high-power diode laser: Precision Engineering, v. 34, no. 3, p. 446–452.

Hofmann, U., T. Wantoch, G. Eberhardt, I. Kinski, M. Moeser, F. Senger, and C. Mallas, 2016, Dynamic shaping of the basic intensity profile of adaptive laser headlights based on resonant MEMS scanning mirrors.

Klocke, F., M. Schulz, , and S. Gräfe, 2017, Optimization of the Laser Hardening Process by Adapting the Intensity Distribution to Generate a Top-hat Temperature Distribution Using Freeform Optics: Coatings, v. 7, no. 6, p. 77.

Klocke, F., M. Schulz, S. Gräfe, and G. Zheng 2017, Laser Hardening of Thin Walled Parts with Cryogenic Cooling, Lasers in manufacturing

Kostov, V., and A. Wanner, Untersuchungen zur zeitaufgelösten Spannungsentwicklung und Eigenspannungsentstehung beim Laserstrahlstandhärten am Beispiel des Stahls 42CrMo4, Karlsruhe, Karlsruher Institut für Technologie (KIT), Diss., 2014, Karlsruhe.

Küpper, F., Entwicklung eines industriellen Verfahrens zur Fest-Phasen-Härtung von Langprodukten mit CO2-Laserstrahlung, Zugl.: Aachen, Techn. Hochsch., Diss., 1996, Aachen, 138p.

Laskin, A., and V. Laskin, 2014, Freeform beam shaping for high-power multimode lasers. in A. V. Kudryashov, A. H. Paxton, V. S. Ilchenko, L. Aschke, and K. Washio, eds., Freeform Beam Shaping for High-Power Multimode Lasers: SPIE Proceedings, SPIE, 1-12.

Leung, M. K.H., H. C. Man, and J. K. Yu, 2007, Theoretical and experimental studies on laser transformation hardening of steel by customized beam: International Journal of Heat and Mass Transfer, v. 50, 23-24, p. 4600–4606.

Martínez, S., A. Lamikiz, E. Ukar, I. Tabernero, and I. Arrizubieta, 2016, Control loop tuning by thermal simulation applied to the laser transformation hardening with scanning optics process: Applied Thermal Engineering, v. 98, p. 49–60.

Noden, S. C., 2000, The application of diffractive optical elements in high power laser materials processing, Loughborough University of Technology, 1-349.

Orlich, J., A. Rose, and P. Wiest, 1973, Zeit - Temperatur - Austenitisierung - Schaubilder: Düsseldorf, Verl. Stahleisen, 264 S.

Primartomo, A., 2005, Laser surface treatment using customised heat source profiles, Dissertation, Loughborough, 1-209.

Pütsch, O., P. Loosen, and R. Schmitt, 2016, Aktive und adaptive Strahlformungssysteme für die Werkstoffbearbeitung mit Laserstrahlung, Dissertation.

Römer, G.R.B.E., and A. J. Huis in 't Veld, 2010, Matlab Laser Toolbox: Physics Procedia, v. 5, p. 413–419.

Sandven, O. A., 1991, Laser Surface Hardening. in A. I. H.M. Committee, ed., ASM handbook: Heat treating: ASM Handbook, ASM International, p. 286–295.

Schmitz-Justen, C., Einordnung des Laserstrahlhärtens in die fertigungstechnische Praxis, Aachen, Techn. Hochsch., Diss., 1986, 146p.

Sundqvist, J., A.F.H. Kaplan, L. Shachaf, and C. Kong, 2017, Analytical heat conduction modelling for shaped laser beams: Journal of Materials Processing Technology, v. 247, p. 48–54.

Völl, A., J. Stollenwerk, and P. Loosen, 2016, Computing specific intensity distributions for laser material processing by solving an inverse heat conduction problem. in F. Dorsch, and S. Kaierle, eds., SPIE 2016 Proceedings: SPIE Proceedings, SPIE, p. 974105.

Wellburn, D., S. Shang, S. Y. Wang, Y. Z. Sun, J. Cheng, J. Liang, and C. S. Liu, 2014, Variable beam intensity profile shaping for layer uniformity control in laser hardening applications: International Journal of Heat and Mass Transfer, v. 79, p. 189–200.